AD-A242 084

‖‖‖‖‖‖‖‖‖‖‖
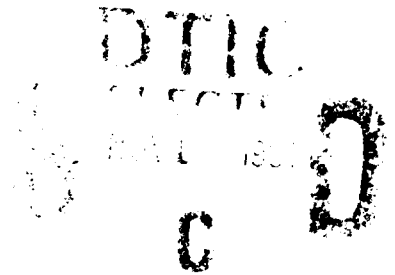
PL-TR-91-2046

SURFACE RESPONSE TO CLOUD SHADOWING

A. Berk
D. C. Robertson
P. K. Acharya

Spectral Sciences, Inc
99 South Bedford Street, #7
Burlington, MA 01803-5169

20 February 1991

Scientific Report No. 3

91-14730

‖‖‖‖‖‖‖‖‖‖‖

This technical report has been reviewed and is approved for publication.

_____   _____
DEAN F. KIMBALL   DONALD E. BEDO, Chief
Contract Manager   Electro-Optical Measurements Branch
Simulation Branch   Optical Environment Division

_____
ALAN D. BLACKBURN, Col, USAF, Director
Optical Environment Division

REPORT DOCUMENTATION PAGE

1a. REPORT SECURITY CLASSIFICATION UNCLASSIFIED	1b. RESTRICTIVE MARKINGS N/A
2a. SECURITY CLASSIFICATION AUTHORITY UNCLASSIFIED	3. DISTRIBUTION / AVAILABILITY OF REPORT Approved for public release; distribution unlimited.
2b. DECLASSIFICATION / DOWNGRADING SCHEDULE • N/A	

4. PERFORMING ORGANIZATION REPORT NUMBER(S) SSI-TR-184	5. MONITORING ORGANIZATION REPORT NUMBER(S) PL-TR-91-2046

6a. NAME OF PERFORMING ORGANIZATION Spectral Sciences, Inc.	6b. OFFICE SYMBOL (If applicable)	7a. NAME OF MONITORING ORGANIZATION Phillips Laboratory
6c. ADDRESS (City, State, and ZIP Code) 99 South Bedford Street, #7 Burlington, MA 01803-5169		7b. ADDRESS (City, State, and ZIP Code) Hanscom AFB, MA 01731-5000

8a. NAME OF FUNDING / SPONSORING ORGANIZATION	8b. OFFICE SYMBOL (If applicable)	9. PROCUREMENT INSTRUMENT IDENTIFICATION NUMBER F19628-89-C-0128
8c. ADDRESS (City, State, and ZIP Code)		10. SOURCE OF FUNDING NUMBERS

PROGRAM ELEMENT NO.	PROJECT NO.	TASK NO.	WORK UNIT ACCESSION NO
62101F	3054	02	AJ

11. TITLE (Include Security Classification)

Surface Response to Cloud Shadowing

12. PERSONAL AUTHOR(S)
A. Berk, D. C. Robertson, and P. K. Acharya

13a. TYPE OF REPORT Scientific No. 3	13b. TIME COVERED FROM 10/89 TO 12/90	14. DATE OF REPORT (Year, Month, Day) 91FEB20	15. PAGE COUNT 34

16. SUPPLEMENTARY NOTATION

17. COSATI CODES			18. SUBJECT TERMS (Continue on reverse if necessary and identify by block number)
FIELD	GROUP	SUB-GROUP	Clouds Soil Energy Budget Heat Flow IR Radiation Boundary Layer

19. ABSTRACT (Continue on reverse if necessary and identify by block number)

This study investigated the response of surface temperature to cloud shadows. A quantitative model applicable to IR backgrounds was developed. Time-dependent heat flow and energy budget equations have been solved to determine the diurnal variation in surface ground temperatures for a dry, sandy soil with a simple vegetation layer under various cloud conditions. Ground temperatures were determined to vary up to 2K in the first minute following cloud shadowing of solar illumination; stable soil temperatures were not reached after over an hour of shade. These results indicate the importance of including cloud shadowing in the SWOE background model.

20 DISTRIBUTION / AVAILABILITY OF ABSTRACT ☑ UNCLASSIFIED/UNLIMITED ☐ SAME AS RPT. ☐ DTIC USERS	21. ABSTRACT SECURITY CLASSIFICATION UNCLASSIFIED
22a. NAME OF RESPONSIBLE INDIVIDUAL Dean Kimball	22b. TELEPHONE (Include Area Code) (617) 377-3642 22c. OFFICE SYMBOL PL/OPB

DD FORM 1473, 84 MAR   83 APR edition may be used until exhausted.   SECURITY CLASSIFICATION OF THIS PAGE
All other editions are obsolete.

TABLE OF CONTENTS

Accession For

NTIS GRA&I   ☑
DTIC TAB   ☐
Unannounced   ☐
Justification

By
Distribution/

Availability Codes

Dist   Avail and/or
          Special

A-1

iii

LIST OF FIGURES

LIST OF FIGURES (Continued)

LIST OF TABLES

1. EXECUTIVE SUMMARY

A goal of the Balanced Technology Initiative (BTI) on Smart Weapons Operability Enhancement (SWOE) is to model the infrared (IR) radiant field from complex natural backgrounds. The degree of realism and model detail must be commensurate with the spatial and temporal resolution of operational and developmental sensors. Thus, the background model with its various scene elements must treat the basic phenomena affecting the radiation signature to the required resolution.

The overall goal of this Spectral Sciences, Inc. (SSI) effort is to provide a preliminary study that quantifies the effect of cloud shadows on surface IR radiance and thereby helps determine the importance of including shadowing in the SWOE model. The diurnal variation of surface ground temperature has been modeled for an "ideal" dry sandy soil with 12 cm vegetation and covered by various stationary cloud fields. Changing cloud shadows result from the sun's movement across the sky. The information resulting from this study includes (1) ground temperature response to shadowing by finite clouds and (2) diurnal ground temperature dependence on fractional cloud cover.

The general approach for determining ground temperature involves three steps:

- ATMOSPHERIC RADIANCE: MODTRAN[1,2] with its multiple scattering option is run to compute the diurnal variation of downward radiant flux and solar illumination for cloud-free and semi-infinite cloud conditions;

- CLOUD SHADOWING: Cloud fields consisting of regularly spaced prolate ellipsoidal clouds are constructed, and the temporal variation of solar illumination is determined; and

- SURFACE TEMPERATURE: The above information is input to a time-dependent energy model for soil terrains with a simple vegetation layer to determine surface temperature.

Figure 1 illustrates the computed variation in ground temperature for 40% cover by 2.4-3.0 km altitude clouds. The model is run for at least one full day to reduce the bias created by initialization of the soil temperature profile. As a general trend, the ground warms after sunrise ($\approx$4:30 a.m. on June 25 at Hanscom AFB) and cools during late afternoon and into the night. The interesting features in this curve are the sharp rises and drops which
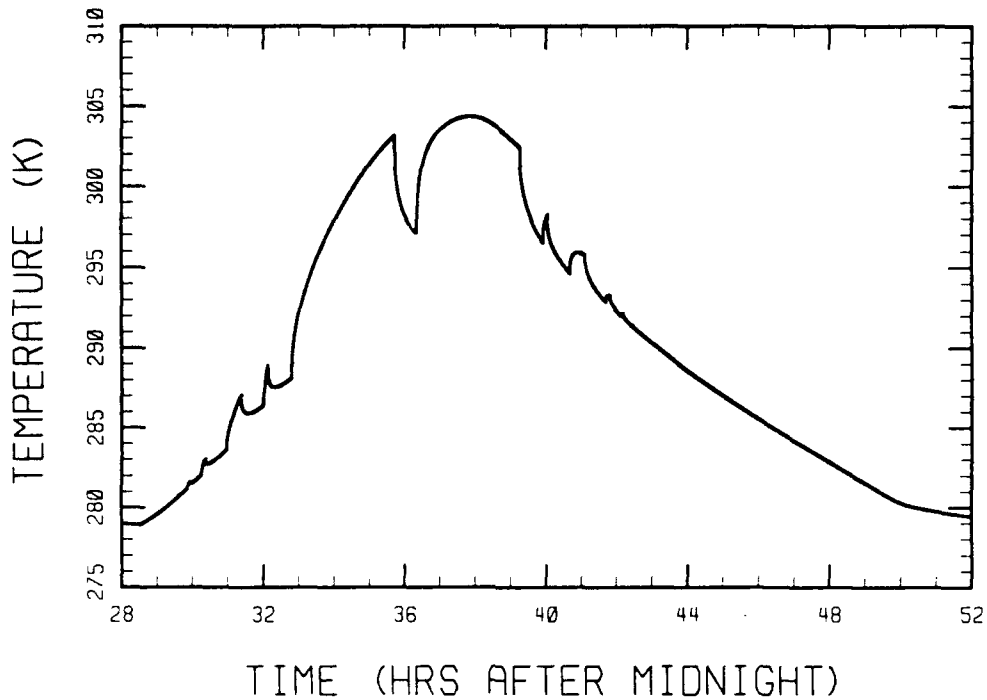
Figure 1. Diurnal Variation of Ground Temperature for 70% Cover by Finite Clouds Between 2.4 and 3.0 km Altitude.

correspond to breaks in the cloud cover. The discontinuities in solar irradiance produce changes of up to 2K in one minute, and, within ten minutes, the ground temperature changes by more than 4K.

The model also predicts the different ground temperature histories that arise from varying cloud cover while keeping all other model inputs constant. Curves of ground temperature for 10, 40, 70, and 100% cover by 2.4-3.0 km clouds were computed relative to the cloud-free ground temperatures; the results for a 24 hour period are shown in Figure 2. For dry, sandy soil, full cloud cover reduces ground temperature by more than 10°C at midday and increases the night temperature in excess of 1°C. For fractional cloud covers, the early morning ground temperatures vary smoothly between the clear sky and complete cloud cover limits. This is not the case during the day. The ground temperature responds quickly to the abrupt changes in solar illumination. Figure 2 also illustrates that the limiting, stable ground temperatures are approached quite slowly. Consider, for example, the 40% cloud cover curve between 36.3 and 39.3 hours after midnight. During this entire period, the ground is solar illuminated and the
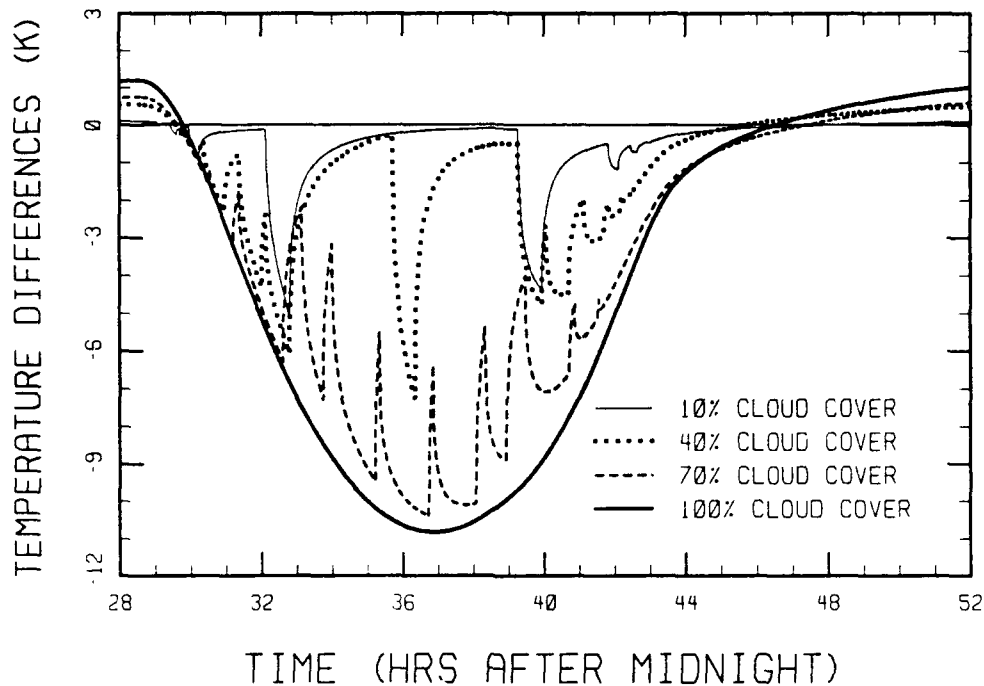
Figure 2. Ground Temperature Differences Between Cloud and No Cloud Scenarios. The Cloud Field is Constructed from Regularly Spaced Prolate Ellipsoidal Clouds Between 2.4 and 3.0 km Altitude.

skyshine is essentially the same as the cloud-free case. Even so, over two hours pass before the ground temperature is stabilized. Thus, the model indicates that although the surface reacts quickly to changes in solar illumination, the sub-surface layers react quite slowly.

The major results of this work are a quantitative verification that cloud shadowing significantly affects the radiant field from complex natural backgrounds and that predictive modeling can describe the temporal and spatial responses of the soil surface temperature. Thus, this study demonstrates the necessity of including cloud shadowing in the SWOE scene model. This effort has also produced a series of modules which can serve as a basis for development of a comprehensive cloud shadowing model. Model upgrades and validation will be needed to insure that SWOE performance requirements are met.

2. CLOUD SHADOWING MODEL

In order to quantify the importance of cloud shadowing for the SWOE natural background model, SSI has developed a preliminary cloud shadowing model. The model consists of three modules:

- DIURNAL - Calculates the diurnal variation of radiation flux incident on the ground,

- CLOUDS - Constructs cloud fields and determines direct solar transmittance, and

- TERRAIN - Solves a time-dependent energy budget equation for surface temperature.

The following subsections discuss the details of these models, their implementation, and results.

Surface temperature predictions due to cloud shadows are naturally very sensitive to input physical conditions. Table I is a complete list of model parameters. The model includes *diurnal variations in solar irradiance and scattering*, and calculations were performed for differing cloud conditions. Since this preliminary study is to demonstrate quantitatively the effect of changing cloud cover on the radiation signature, representative soil and vegetation parameters were chosen to correspond to a scenario in which the temperature response is expected to be accentuated. The vegetation parameters correspond to summer barley, and surface conditions reflect a fairly dry and sandy soil.

2.1 Diurnal

DIURNAL is a driver routine which repeatedly calls MODTRAN[1,2] to determine the diurnal variation in solar irradiance and downward flux of skyshine radiation on the ground. Inputs include a reference MODTRAN input stream along with time step information. Beginning at sunrise, DIURNAL executes MODTRAN at each time step with solar direc ion and flux determined by time of day, day of year, longitude and latitude.

The only difference between the MODTRAN input streams, other than time of day, is an adjustment made to the reference temperature and water vapor profiles in the boundary layer (<0.15 km) to insure consistency with surface values. Following Barnett,[3] diurnal variations in surface (1.5 m above ground) temperature, T, and relative humidity, R, are parameterized in the cloud shadowing model, with extreme values occurring at sunrise, t_s, and 2:00 p.m.:

TABLE I.   CLOUD SHADOWING MODEL INPUT PARAMETERS

EXTRA-TERRESTRIAL SOLAR IRRADIANCE	
Flux	Calculated by MODTRAN for day 176 (June 25)
Direction	Calculated every 20 minutes on day 176 at 42°28'N, 71°17'W (MODTRAN)

ATMOSPHERE	
T, P & Molecular Profiles	US STANDARD
Aerosol Profile	23 km Visibility Rural Extinction Model (MODTRAN)

CLOUD FIELD	
Distribution	Regularly Spaced Prolate Ellipsoidal Clouds at 0.7 and 2.7 km Altitude
Absorption	MODTRAN STRATUS and ALTOSTRATUS Models
Scattering	MODTRAN STRATUS and ALTOSTRATUS Models

BOUNDARY LAYER (1.5 m above ground averages)	
Wind Speed	2.0 m/s
Air Temperature	Varies Smoothly between 278 and 300 K
Relative Humidity	Varies Smoothly between 40 and 45%

VEGETATION	
Fractional Cover	0.3
Long Wave Emissivity	0.95
Short Wave Albedo	0.20
Height	0.12 m

SOIL	
Initial Temperatures	Evenly Spaced between Surface Air Temperature and 290K at 1 m Depth
Conductivity	1.1 W m^{-1} K^{-1}
Diffusivity	0.004 cm^2/s
Saturation	25%
Heat Transfer Coefficient	0.012
Long Wave Emissivity	0.95
Short Wave Albedo	0.35

$$T = T_0 \qquad\qquad 2 \le t \le t_s \qquad (1)$$

$$T = T_0 + \Delta T \sin(\frac{\pi}{2} \frac{t-t_s}{14-t_s}) \qquad\qquad t_s \le t \le 14 \qquad (2)$$

$$T = (T_0 + \Delta T)^{(26-t)/12} T_0^{(t-14)/12} \qquad\qquad 14 \le t \le 26 \qquad (3)$$

$$R = R_0 \qquad\qquad 2 \le t \le t_s \qquad (4)$$

$$R = R_0 - \Delta R \, \sin(\frac{\pi}{2} \, \frac{t - t_s}{14 - t_s}) \qquad\qquad t_s \leq t \leq 28 - t_s \qquad (5)$$

$$R = R_0 \qquad\qquad 28 - t_s \leq t \leq 26 \qquad (6)$$

where t is the local time in hours after midnight (2 to 26), T_0 and R_0 are the temperature and relative humidity, respectively, at sunrise, ΔT and ΔR are the diurnal range of temperature and relative humidity, respectively, and sunrise is assumed to occur a minimum of two hours after midnight.

The five separate MODTRAN runs which are performed at each time step are:

- Clear Sky Direct Solar Irradiance,

- Clear Sky Short-Wave (0.3-3.3 μm) Skyshine,

- Clear Sky Long-Wave (3.3-200.0 μm) Skyshine,

- Clouded Sky Short-Wave (0.3-3.3 μm) Skyshine, and

- Clouded Sky Long-Wave (3.3-200.0 μm) Skyshine.

MODTRAN has been modified to output skyshine (downward radiant flux) which is calculated as part of the multiple scattering routine. Separate calculations are performed in the long- and short-wave to accommodate different surface albedos. The DIURNAL assumption that the surface albedo is independent of both angle and wavelength within each spectral region is consistent with the present version of the energy budget model. Cloud calculations for determining skyshine assume 100% cloud cover. Since skyshine is a fairly diffuse source, the cloud shadowing module interpolates the downward radiant flux between the clear sky and 100% cloud cover limits for input to the energy budget.

The DIURNAL calculations were performed for an observer located at Hanscom AFB (42°28'N, 71°17'W), Table I. Radiation flux was determined each twenty minutes for a 24 hour period starting from sunrise ($\approx$4:30 a.m.) on day 176 (June 25). The results were interpolated temporally for input into the heat flow equation (Subsection 2.3). The 1976 US Standard atmosphere and the MODTRAN 23 km visibility rural extinction aerosol model defined atmospheric conditions. Predictions for two cloud types, low altitude stratus (0.33-1.00 km) and mid altitude altostratus (2.4-3.0 km),[4] were calculated.

- 6 -

Surface irradiances from the DIURNAL calculations are illustrated in Figure 3. A number of observations are noteworthy:

- At the maximum in the cloud-free sky solar irradiance curve, corresponding to a 19° zenith angle, almost 60% of the incident flux is transmitted directly. With complete cloud cover, essentially no unscattered solar radiation reaches the ground.

- At night, the downward radiation flux is enhanced by both the emission of thermal energy by clouds and the clouds' reflection of earth's thermal emission. For warm, low altitude clouds, this effect is greatest.

- Solar scatter contributes to skyshine during the day. Thin clouds tend to increase the amount of solar radiation scattered downward, but as the cloud optical depth becomes large, most solar radiation is either reflected upward or absorbed. Since MODTRAN extinction coefficients for stratus clouds are approximately 60% of those for altostratus, the stratus clouds lead to a greater contribution from solar scatter.[5]

- During early morning and late afternoon, cloud depth along the solar path becomes quite large, and the solar scatter contribution to skyshine drops. In fact, the total skyshine for altostratus clouds is below the clear sky value between 5:50 and 9:30 a.m., and again between 2:30 and 6:10 p.m.
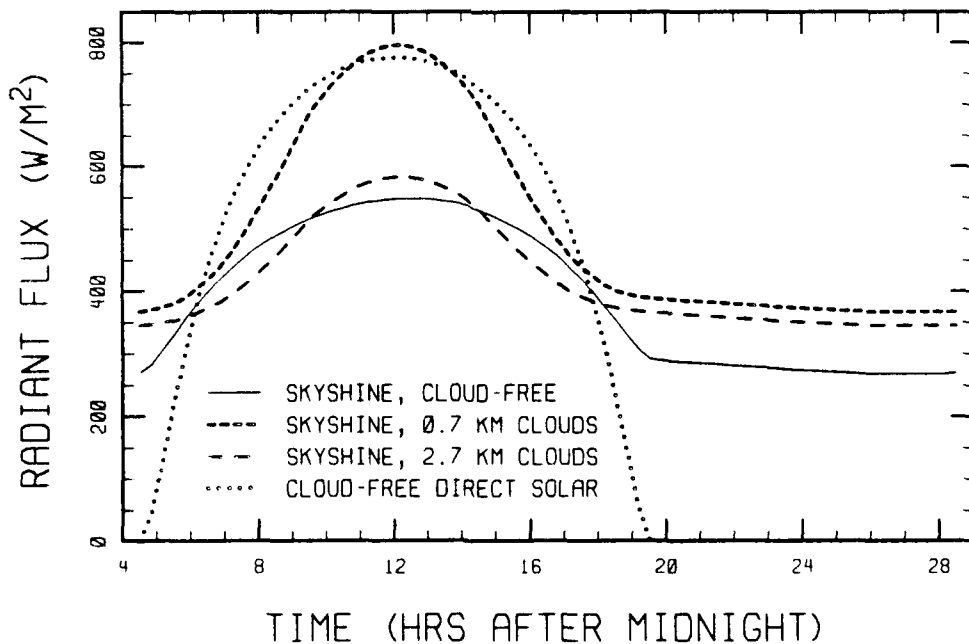

Figure 3. Diurnal Variation of Surface Irradiance Components Calculated by DIURNAL. Skyshine Includes Scattered Solar. The Dashed Curves Include Complete Cover by Stratus (0.33-1.00 km altitude) and Altostratus (2.4-3.0 km Altitude) Clouds. The Predictions are for an Observer at Hanscom AFB on Day 176.

- At midday, the total skyshine contribution from the clouds at 0.7 km altitude actually exceeds the clear sky direct solar component. Of course, this does not mean the clouded sky is warmer than the cloud-free sky; the total downward flux in the cloud-free sky scenario is the sum of the solar irradiance (776 W/m^2) and skyshine (548 W/m^2) contributions, which are considerably more than the stratus cloud skyshine (796 W/m^2).

2.2 Clouds

The routine CLOUDS determines the diurnal variation in transmittance of direct solar irradiance through a stationary cloud field. For this study, cloud fields were defined as a lattice of prolate ellipsoidal clouds, each centered at a fixed altitude above the curved earth and oriented so that the local vertical is parallel to the major semi-axis. Figure 4 is a polar plot illustration of the cloud field as seen by a ground observer. In this cloud lattice, the observer always has a cloud directly overhead. The figure was generated for 40% cover by clouds of width, base and top equal to 1.0, 2.4, and 3.0 km, respectively. (Throughout this report, cloud cover is defined as the percentage of the earth's surface for which clouds are directly overhead; this is different from the percent of blue sky blocked by clouds from a ground observer's perspective.) Figure 4 is equivalent to an all-sky image; the radial distance from the center is proportional to zenith angle with the edge corresponding to the horizon, and the azimuthal angle is defined relative to the compass directions. The periodic cloud structure was selected to lessen the severity of the assumption that skyshine can be interpolated between the cloud-free and 100% cloud cover limits.

Additional simplifying assumptions were instituted in this preliminary cloud shadowing model. The sun is treated as a point source, and the clouds are homogeneous. Initially, optical properties for the finite cloud were defined with the MODTRAN model, and transmittances were calculated with the SSI cloud model. The CLOUDS module calculates the diurnal variation of geometric cloud depth along the solar path, as shown in Figures 5 and 6. Since cloud extinction coefficients are so large in the short wave (> 88 km^{-1} for altostratus and > 53 km^{-1} for stratus[4]), the transmittance rapidly falls to zero whenever clouds intercept the solar path. Therefore, the spectral integral over the product of solar irradiance and cloud transmittance was eliminated, and the solar irradiance set to zero whenever clouds intersect the solar path to the ground.
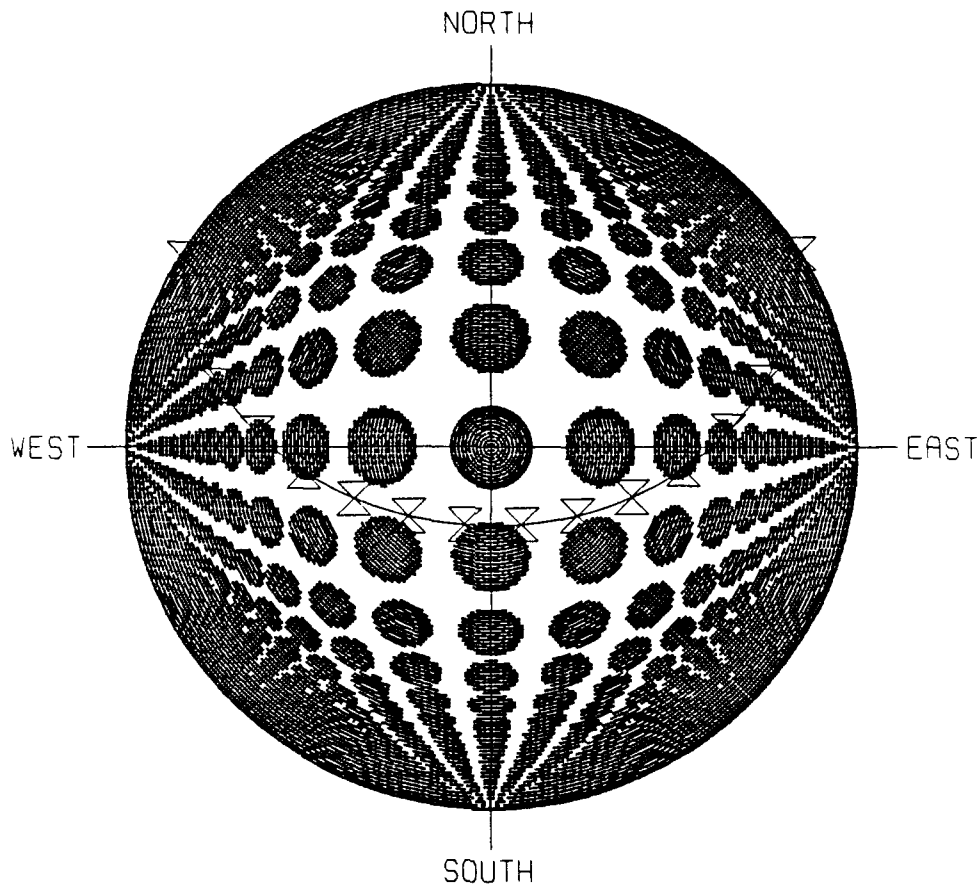
Figure 4. Schematic Illustrating the Stationary Cloud Field. The Polar Plot Solar Trajectory is for a Ground Observer Located 42°28'N, 71°17'W on Day 176. Distance from Center is Proportional to Zenith Angle with the Edge Representing the Horizon. Cloud Cover is 40% and the Clouds are Prolate Ellipsoids with Base = 2.4 km, Top = 3.0 km, and Width = 1.0 km. Hour Glasses are Drawn Each Hour Past Sunrise with Sunrise Beginning in the East at 4:30 a.m. Local Time.

A lattice structure for the cloud fields was chosen in order to be more consistent with the semi-infinite clouds used to calculate the skyshine irradiance. The MODTRAN altostratus cloud model has a base of 2.4 km and top of 3.0 km; the values for the low altitude stratus are 0.33 km and 1.00 km, respectively. All clouds were given a width, W, of one kilometer. The distance between nearest neighbor clouds, D, was calculated from the equation

$$D = \frac{W}{2} \sqrt{\pi/F} \quad , \tag{7}$$

Figure 5. Diurnal Variation of Geometric Cloud Depth Along the Solar Path for Three Fractional Covers of Clouds at 2.4 km. The Cloud Scene Consists of a Square Lattice of Prolate Ellipsoidal Clouds Each with Base, Top, and Width Equal to 2.4, 3.0, and 1.0 km, Respectively. The Ground Observer is located 42°28'N, 71°17'W, and Time is Measured from the Beginning of Day 175 (4:00 a.m. to 8:00 p.m. on Day 176 at Hanscom AFB).
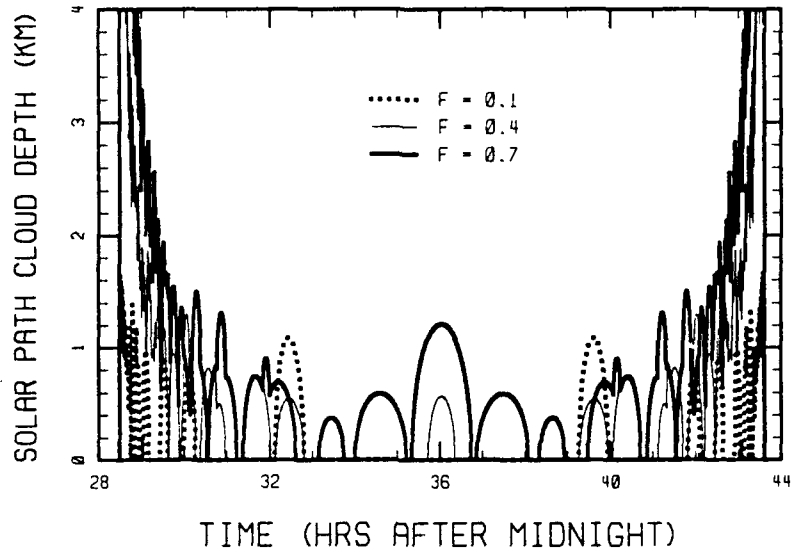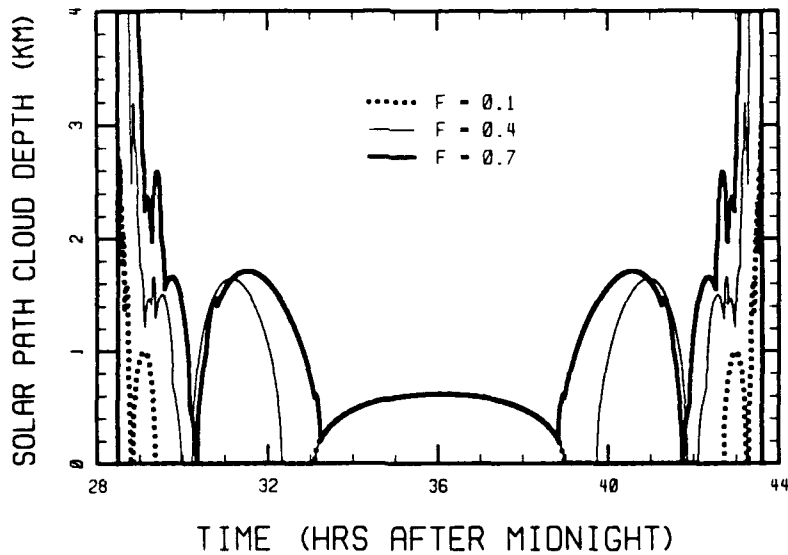

Figure 6. Diurnal Variation of Geometric Cloud Depth Along the Solar Path for Three Fractional Covers of Clouds at 0.33 km and for the Same Conditions as Figure 5.

where F is the fraction of the earth covered by the cloud field. Note that F is smaller than the fraction of sky containing clouds from the perspective of a ground observer. Calculations were performed for F values of 10, 40 and 70%.

Cloud shadowing was modeled for day 176, June 25. The sun's trajectory as seen from the ground at Hanscom AFB is shown in Figure 4. Note that the F=0.4 curve in Figure 5 is indeed zero whenever the solar path passes between clouds in Figure 4. The cloud directly overhead always occults the sun around noon for the low altitude cloud lattice, so the three factional cloud covers in Figure 6 are the same at 36 hours.

2.3   Terrain

Calculations of time-dependent soil/vegetation temperature were performed by the TERRAIN module. This module is based on Deardorff's terrain model[5] with the single additional limitation that the soil moisture content is constant. TERRAIN uses a finite differences approach to solve the one-dimensional heat flow equation below the surface:

$$\frac{\partial T}{\partial t} = K \frac{\partial^2 T}{\partial z^2} \tag{8}$$

where

K = soil thermal diffusivity,
z = depth below the surface,
t = time, and
T = temperature at depth z and time t.

The boundary conditions include (1) an initial (early morning) temperature profile, (2) a constant lower boundary temperature (one meter below the soil surface) and (3) a temporal surface temperature which is determined along with the vegetation temperature from a pair of energy budget equations:

$$S_s + R_s + H_s + E_s + G_s = 0 \tag{9}$$

$$S_v + R_v + H_v + E_v \qquad = 0 \tag{10}$$

where

S = Short wave (solar) illumination,
R = Net Long wave (thermal) radiation,
H = Sensible heat exchange,
E = Evapotranspiration heat exchange, and
G = Conductive transfer to the soil.

Subscripts s and v refer to soil and vegetation, respectively.

Beginning with an initial temperature profile for the 501 homogeneous soil layer boundaries, TERRAIN increments in time, solves the heat flow equation to determine the temperature profile below the surface (every 3 seconds), and then uses the energy budget equations to determine the soil and vegetation temperature (every 15 seconds). The model is run for 2 days with results for the second day reported; the first day allows the soil temperature profile to converge to its periodic limit. Inputs to the model include the time dependent skyshine and solar irradiance from the DIURNAL and CLOUDS modules along with the boundary layer, vegetation and soil parameters listed in Table I.

To maximize the temperature response, a fairly dry, sandy soil was selected. Low moisture content and air pockets lower the overall conductivity, and the low moisture content also decreases evapotranspiration. The net effect is that absorbed radiation has no quick outlet and therefore produces rapid temperature changes. The soil parameters in Table I are based on averages listed in the first two chapters of Boundary Layer Climates.[6] Soil moisture, although low (25% of saturation), is in the acceptable range for plant growth.[6] The bare soil heat transfer coefficient, c, is calculated from

$$c = \frac{k^2}{[\ln(z/z_0)]^2} \tag{11}$$

where k is the von Karmon constant (0.4), z is the altitude of the surface wind speed measurement (1.5 m) and z_0 is the roughness length (0.0016 m used here; compare Table 2.2 of Reference 6).

Deardorff's model[5] allows for introduction of a simple vegetation layer. Vegetation height and fractional cover have been assigned values appropriate for summer barley.[5,7] The vegetation fractional cover is defined as the area average shielding factor associated with the degree to which foliage prevents short-wave radiation from reaching the ground. Estimates for short wave albedo and long wave emissivity are based on Table 1.1 of Reference 6.

3. CALCULATIONS

Calculations were performed for both altostratus (2.4-3.0 km altitude) and stratus clouds (0.33-1.00 km altitude) with fractional cloud covers of 0, 10, 40, 70 and 100%. Results are discussed the following subsections.

3.1   Surface Energy Budget

Solutions to the energy budget equations show the response of vegetation and soil to changes in incident radiation. In this subsection, four scenarios are considered: foliage and soil energy budgets with no clouds and with 40% cover by the stationary altostratus cloud field.

The diurnal variation of the foliage energy budget is driven by the incident radiation, which consists of solar flux, skyshine and soil thermal emission. Since the coverage for summer barley is only 30%,[5,7] most of the incident flux passes through the vegetation without being absorbed. For clear sky conditions, Figure 7 reveals that the nighttime incident radiation is more than balanced by the vegetation's thermal emission. During the day, both solar illumination and convection from the warm air add energy to the barley. This energy raises the foliage temperature and causes foliage moisture to evaporate.

Cloud shadowing produces sharp changes in the solar irradiance. Figure 8 illustrates the energy budget for 40% cover by altostratus clouds. Each valley in the absorption curve corresponds to a cloud shadow. To compensate for the decrease in incident radiation, foliage thermal emission and water evaporation decrease and sensible heat transfer, i.e., convection from the surrounding air mass, increases. The differences between nighttime absorption in Figures 7 and 8 is less than the differences in Figure 3 because cloud cover is only 40% and the ground is warmer under cloud cover (i.e. greater soil thermal emission).

Figure 9 illustrates the soil energy budget for this cloud-free scenario. An additional flux term, energy conducted through the soil, is present. At night, the top soil is cooler than the lower layers, and upwards conduction plus the downward radiant flux keeps the surface warm. During the day, solar irradiance heats the surface, causing the temperature to rise and reversing the direction of the soil heat flow. Evapotranspiration and convection are of minor importance for the dry, sandy soil under cloud-free conditions.

Changes in the soil energy balance resulting from cloud shadowing are shown in Figure 10. Consider the model predictions between 35 and 37 hours. Within seconds of solar occultation, the surface temperature begins to drop, causing a sharp soil temperature gradient
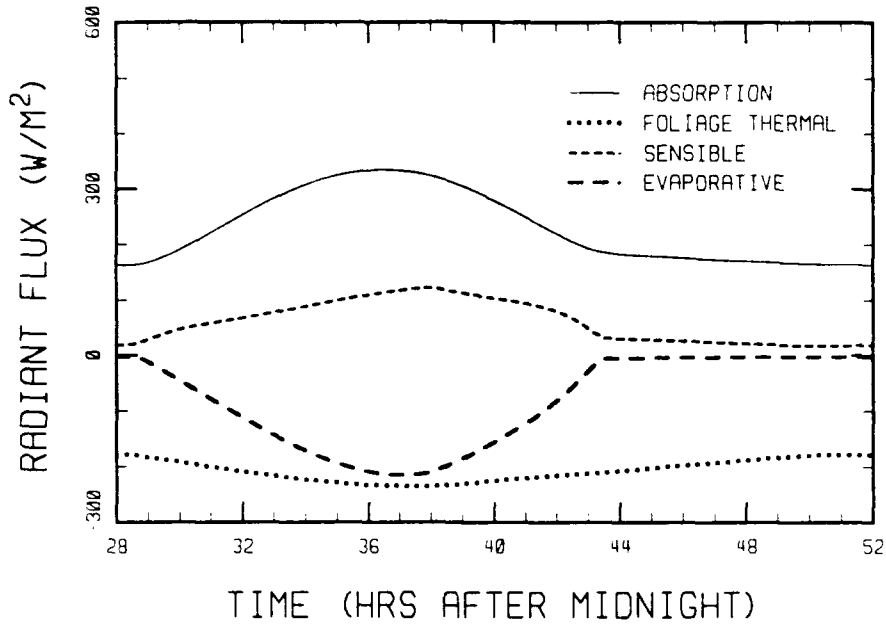
Figure 7. Diurnal Variation of the Cloud-Free Energy Budget for Barley. Absorption Includes Solar Irradiance, Skyshine, and Soil Thermal Emission.
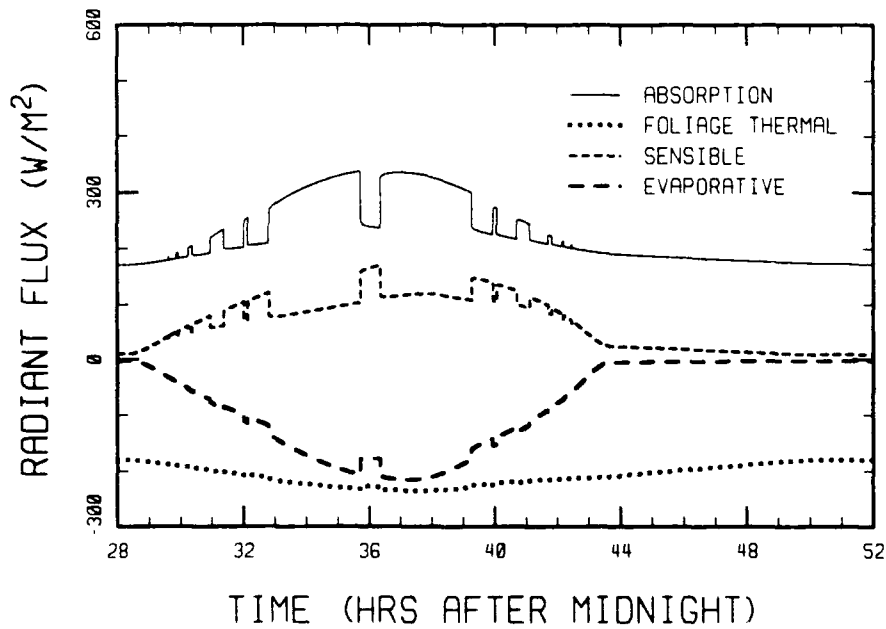

Figure 8. Diurnal Variation of the Barley Energy Budget Under 40% Cover by 2.4-3.0 km Altostratus Clouds. Absorption Includes Solar Irradiance, Skyshine, and Soil Thermal Emission.
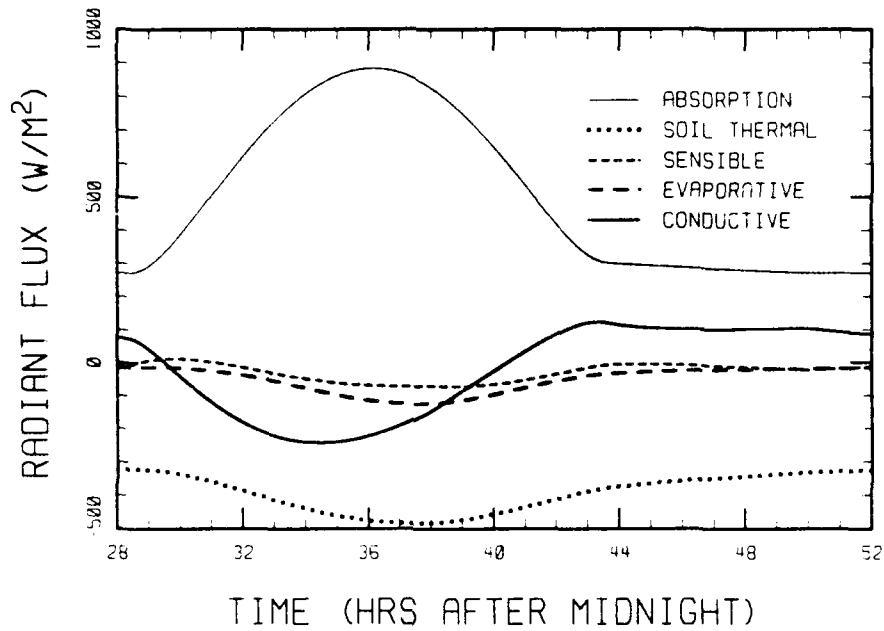
Figure 9. Diurnal Variation of the Cloud-Free Energy Budget for Soil Containing Barley. Absorption Includes Solar Irradiance, Skyshine, and Vegetation Thermal Emission.
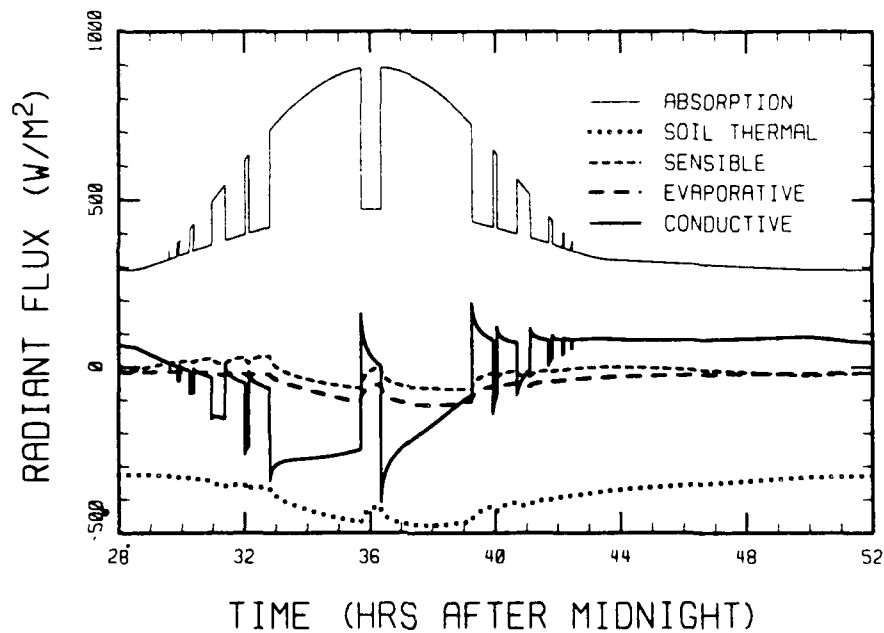

Figure 10. Diurnal Variation of the Energy Budget for Soil Containing Barley and Under 40% Cover by 2.4-3.0 km Altostratus Clouds.

and reversing the direction of heat conduction. As shadowing persists, the temperature continues to drop, but the magnitude of the temperature gradient lessens as the inner soil layers cool. Energy balance is maintained by reducing thermal emission, evapotranspiration and sensible heat transfer. When the sun reappears, essentially the reverse process occurs; a sharp temperature gradient is followed by a reduction in its magnitude and by initiation of response from the other energy components.

3.2 Diurnal Surface Temperatures

The long-wave upward radiant flux, $I^{\uparrow}$, from soil with a simple vegetation layer has the form

$$I^{\uparrow} = (1-\sigma_V) [\epsilon_S \, \sigma \, T_S^4 + (1-\epsilon_S) \, I^{\downarrow}] + \sigma_V [\epsilon_V \, \sigma \, T_V^4 + (1-\epsilon_V) \, I^{\downarrow}] \tag{12}$$

where

$$
\begin{aligned}
\sigma_V &= \text{Fractional Cover of Vegetation,} \\
\epsilon_S &= \text{Soil Surface Emissivity,} \\
\epsilon_V &= \text{Vegetation Emissivity,} \\
T_S &= \text{Soil Surface Temperature,} \\
T_V &= \text{Vegetation Temperature,} \\
\sigma &= \text{Stefan-Boltzmann Constant, and} \\
I^{\downarrow} &= \text{Long-Wave Downward Radiant Flux.}
\end{aligned}
$$

The TERRAIN module calculates soil surface and vegetation temperatures so that scene radiances can be determined.

3.2.1 Cloud-Free Conditions

The TERRAIN model predictions for the diurnal variation of vegetation, soil surface and ground temperatures under cloud-free conditions are shown in Figure 11. The ground temperature has been defined as a weighted average of the soil surface and vegetation temperature

$$T_g = (1-\sigma_V) \, T_S + \sigma_V \, T_V \tag{13}$$

Also shown in Figure 11 is a curve of the surface air temperature, which is input to the model and held constant for these scenarios.

For the cloud-free scenario, the barley temperature is cooler than the surface air at all times with the maximum difference approaching 3K at noon. The barley remains relatively cool because absorption of incident daytime solar radiation is balanced by vaporization of the vegetation's moisture, Figure 7. The soil temperature at sunrise is about 1K above air temperature. As the sun begins to rise, the soil heats up more slowly than the air. Much of the initial solar irradiance acts to warm the inner soil layers. As solar irradiance continues to increase, the soil surface temperature rises more sharply, peaking between noon, the maximum in solar radiation and 2 p.m., the maximum of the air temperature. Cooling is most rapid between 4 and 7 p.m., almost 4K/hour and then slows as the conduction of heat from the inner soil layers becomes influential.

3.2.2 Full Cloud Cover

The major effects of complete cover by 2.4-3.0 km altostratus clouds are to lower the incident radiation during the day by occulting the solar irradiance and to increase the nighttime skyshine by forming a layer of insulation. The barley responds with slightly lower temperatures during the day and slightly warmer temperatures at night, Figure 12. The influence on the vegetation temperature is not large because the solar radiation primarily functions to lessen moisture content and the additional nighttime thermal contributions are balanced by a reduction in convective heating. The soil's response is much more drastic. The maximum soil surface temperature with complete cover by altostratus is 15K less than the cloud-free value. From 2 p.m. to 2 a.m., the soil temperature drops at a relatively slow, almost constant rate of 1K/hour. At sunrise, the soil temperature with full cloud cover is more than 1K warmer than the cloud-free soil temperature - a reversal of over 16K between the cloud-free and full cloud cover scenarios.

3.2.3 Partly Cloudy Conditions

The response of the soil surface and foliage temperatures under partly cloudy conditions with 2.4 - 3.0 km altostratus is illustrated in Figures 13-15. In these curves, the general trend is the same. As soon as the sun is occulted, temperatures drop drastically, and when the sun reappears, temperatures abruptly rise. For vegetation, the model predicts that the full change occurs instantaneously, which illustrates a limitation of the model in its present form. Since
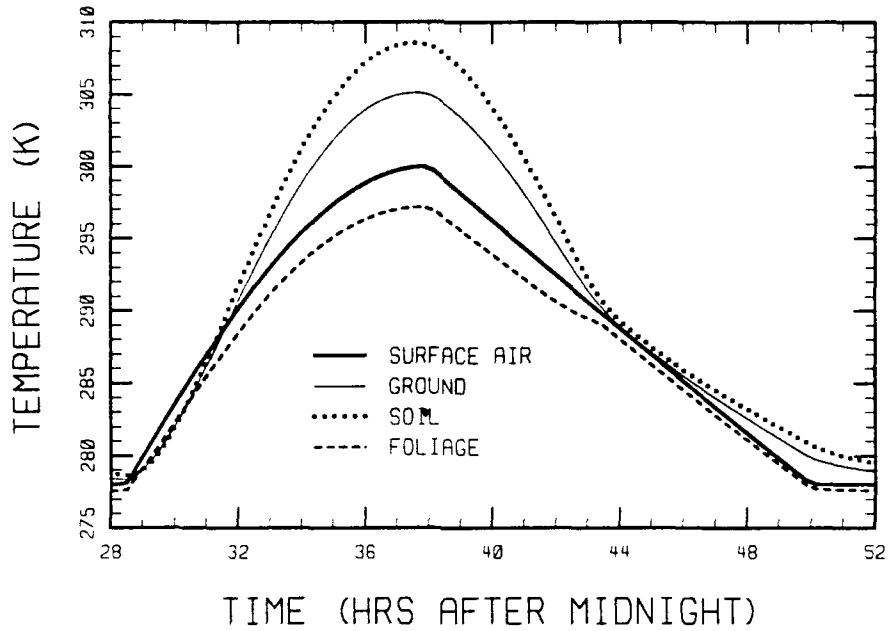
Figure 11. Diurnal Variation of Surface Air, Ground, Surface Soil, and Barley Temperature Under Cloud-Free Conditions.
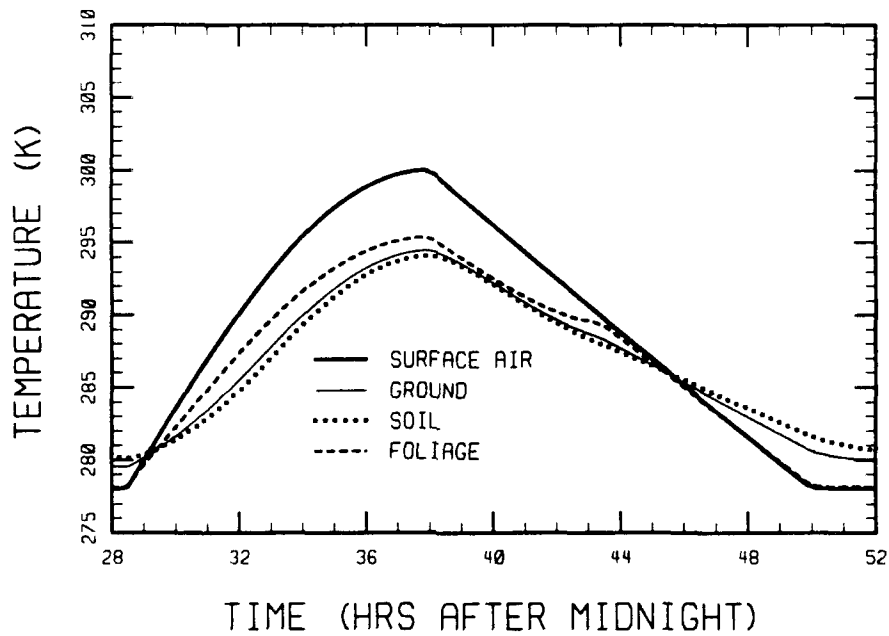

Figure 12. Diurnal Variation of Surface Air, Ground, Surface Soil, and Barley Temperature Under 100% Cover by Altostratus Clouds, 2.4-3.0 km.
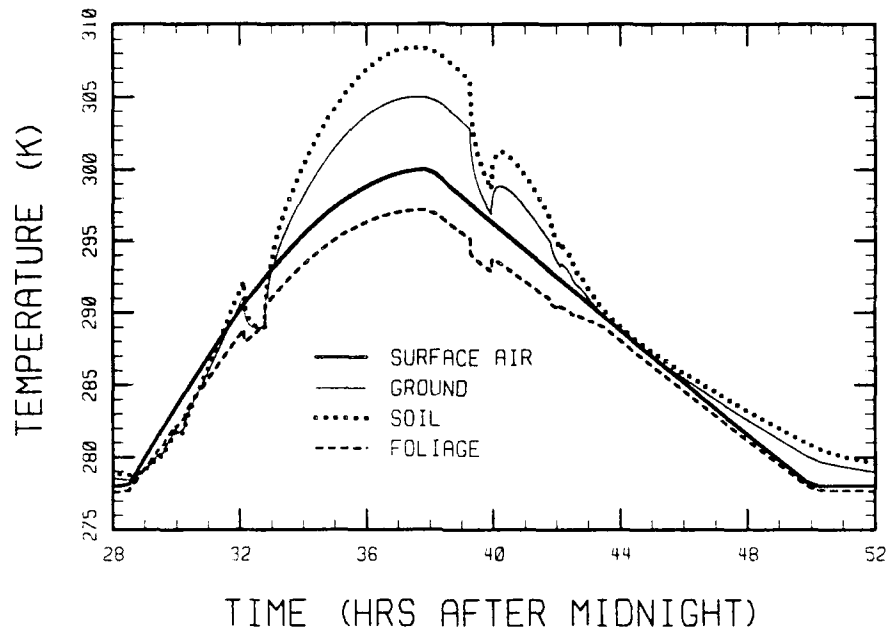
Figure 13. Diurnal Variation of Surface Air, Ground, Surface Soil, and Barley
Temperature Under 10% Cover by Altostratus Clouds, 2.4-3.0 km.
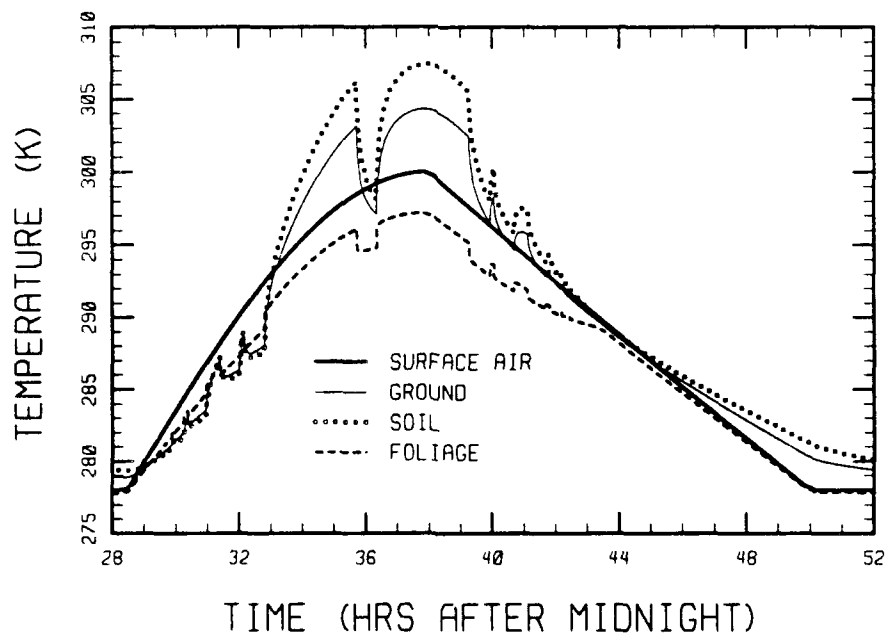
Figure 14. Diurnal Variation of Surface Air, Ground, Surface Soil, and Barley
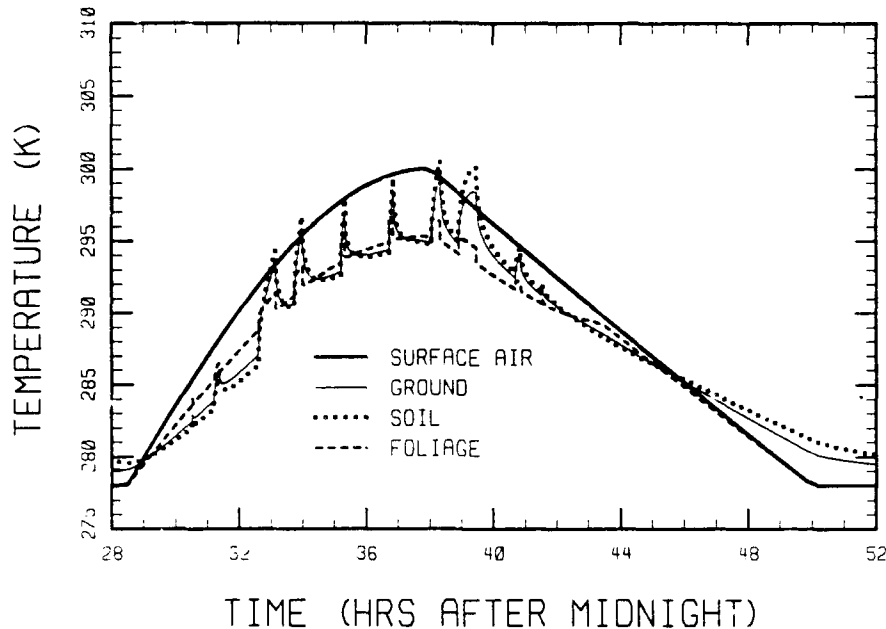Temperature Under 40% Cover by Altostratus Clouds.

Figure 15. Diurnal Variation of Surface Air, Ground, Surface Soil, and Barley Temperature Under 70% Cover by Altostratus Clouds.

foliage is treated as a single layer, there is no mechanism for allowing the heat to properly dissipate downward through the vegetation. For soil surface temperatures, there is also a quick response, but the temperature continues to change for over an hour. Figure 16 shows an enlargement of the 40% cloud cover ground temperature curve between 35.7 and 36.7 hours. The temperature changes by more than 2K in the first minute, and by a full 5K in 30 minutes.

In Figure 17, ground temperatures for 10, 40, 70 and 100% cover by altostratus clouds (2.4-3.0 km) are plotted relative to the cloud-free temperatures. At night, cloud cover provides an insulation for the atmosphere, and by sunrise ground temperature varies smoothly between the clear sky and semi-infinite cloud limits. As seen in Figure 3, the daytime skyshine irradiance from cloud-free and 100% cloud cover by 2.7 km altostratus are almost the same. Since the skyshine under these conditions is relatively independent of cloud cover, daytime temperature variations are driven by the direct solar irradiance, and the ground temperatures oscillate between the cloud cover limits. Figure 17 illustrates the considerable lag time before the soil reaches asymptotic temperatures. After hours of solar illumination, previously shaded ground still has not heated to the clear sky limit. Similarly, regions shaded for over an hour have not cooled to the semi-infinite cloud limit.
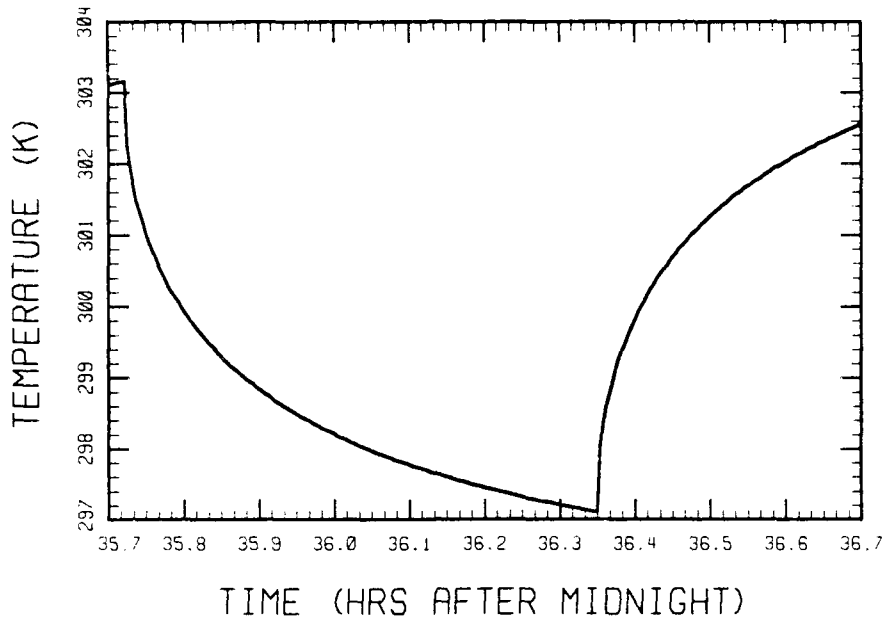
Figure 16.   Enlargement of the Ground Temperature Curve from Figure 14 During the Passing of a Finite Cloud.
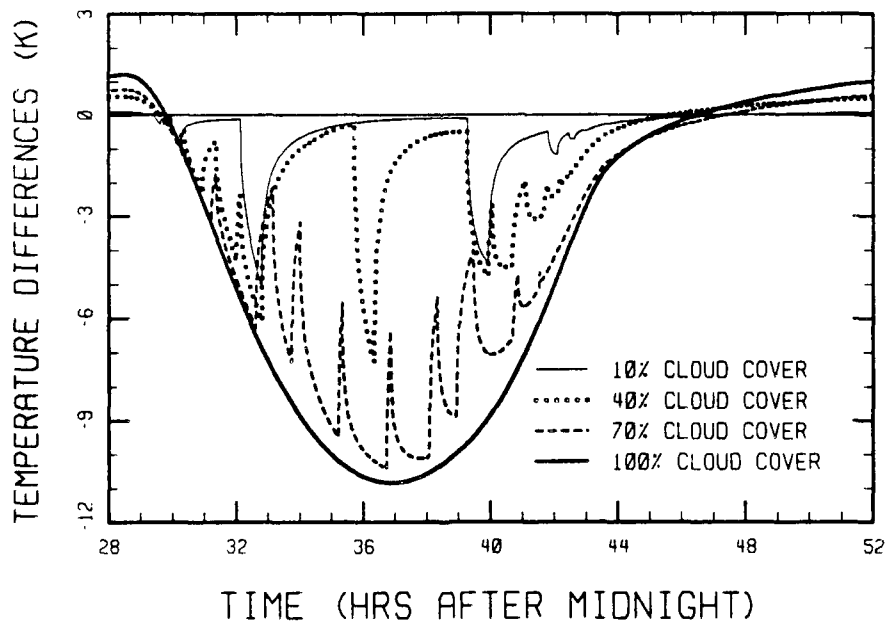

Figure 17.   Differences in Ground Temperatures Between Altostratus (2.4-3.0 km) Clouds of Various Fractional Cover and Cloud-Free Conditions.

3.2.4 Low-Altitude Cloudy Conditions

An additional set of calculations was performed for low-altitude stratus (0.33-1.00 km) clouds. Curves of the diurnal variation in soil surface and summer barley temperature are plotted in Figures 18-21. Two major differences exist between the altostratus and stratus clouds:

- For a given fractional cloud cover, the lower altitude cloud field blocks solar illumination more hours of the day (compare Figures 5 and 6); and

- Skyshine from warm stratus clouds is more intense than that from altostratus (Figure 3).

The first point results from the assumed cloud lattice structure. The net effect of these differences is that the ground under stratus cloud cover is warmer than under altostratus except when solar irradiance has been blocked for an extended period of time by the low clouds. Sudden changes in solar illumination induce abrupt changes in ground temperature (> 1K in the first minute), and the cooling or warming continues at a slower rate for over an hour with a total change in temperature of 3 to 4K.
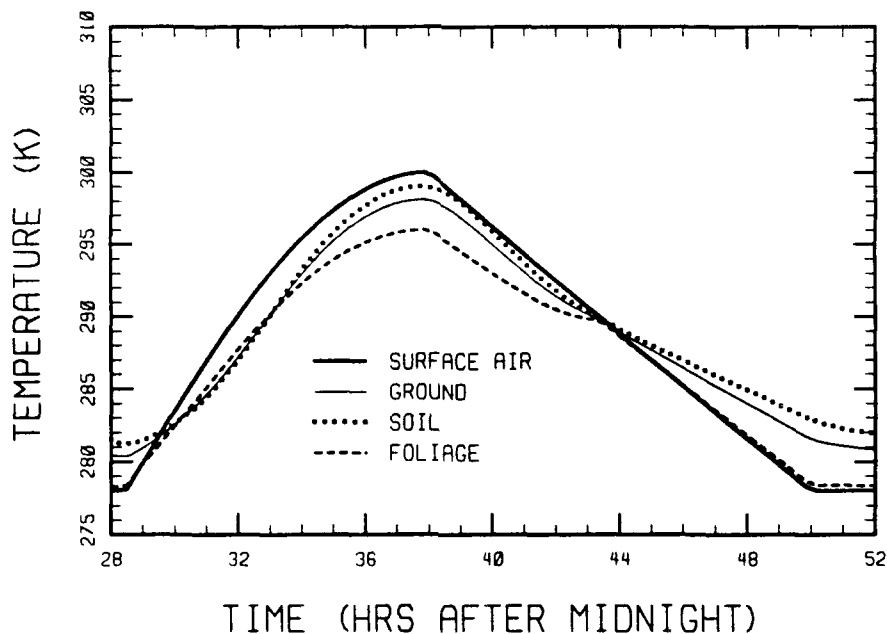

Figure 18. Diurnal Variation of Surface Air, Ground, Surface Soil, and Barley Temperature Under 100% Cover by Stratus Clouds, 0.33-1.00 km.
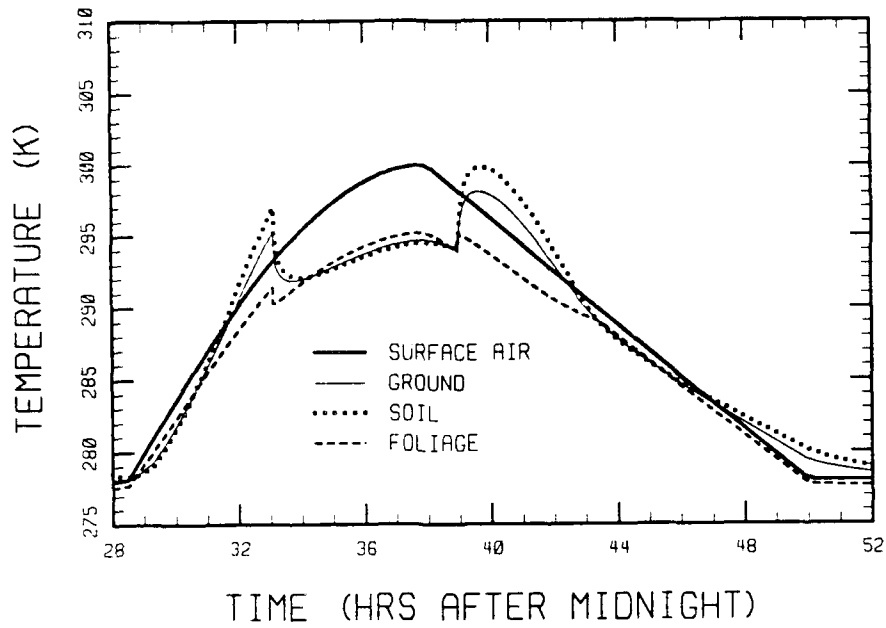
Figure 19. Diurnal Variation of Temperatures Under 10% Cover by Stratus Clouds.
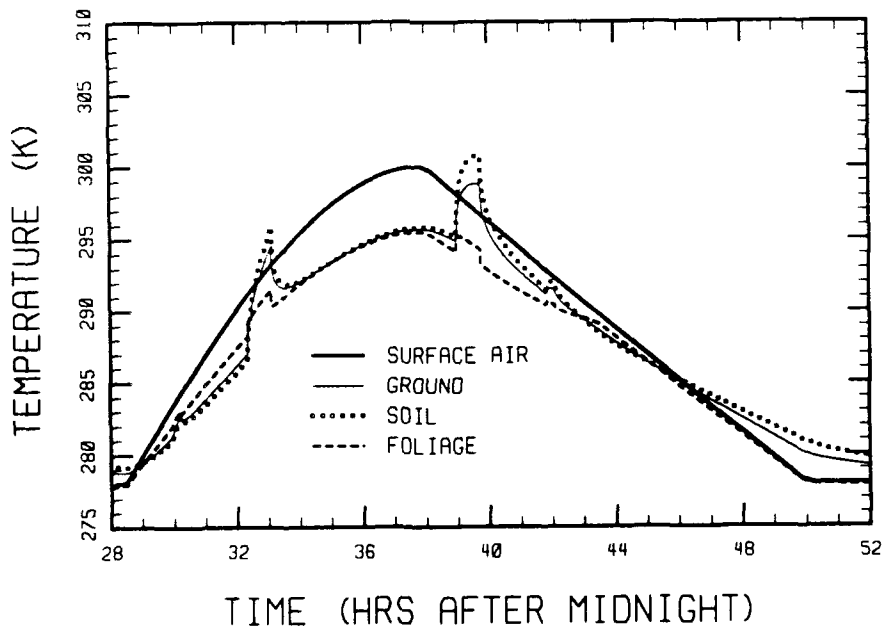

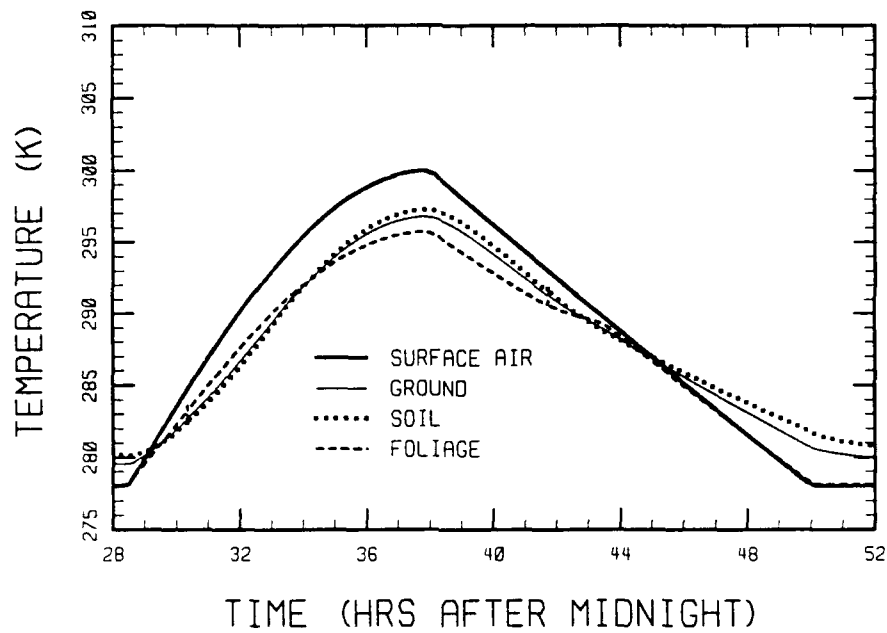Figure 20. Diurnal Variation of Temperatures Under 40% Cover by Stratus Clouds.

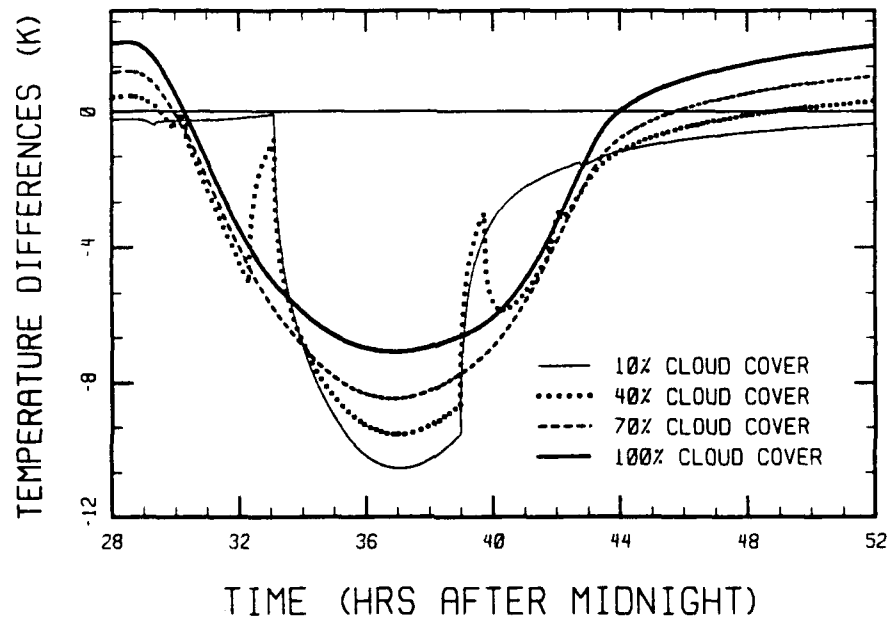Figure 21. Diurnal Variation of Temperatures Under 70% Cover by Stratus Clouds.

Figure 22. Differences in Ground Temperatures Between Stratus Clouds (0.33-1.00 km) and Cloud-Free Conditions.

The effect of the large contribution from skyshine during the day is seen in the temperature difference curves of Figure 22. The ground temperature curves under fractional cover by stratus clouds do not fall between the cloud-free and 100% cloud cover limits, especially during midday. The reason is as follows: The cloud lattice always has a cloud directly overhead which occults the sun between 9 a.m. and 3 p.m., Figure 6. Thus these clouded skies are always cooler than the cloud-free sky. In addition, the skyshine contribution increases with increasing cloud cover. Since the 10% cloud cover curve has the least warming due to skyshine and still has no midday solar illumination, the ground it shadows is coolest.

4. RECOMMENDATIONS

This study has demonstrated the necessity of including cloud shadowing in the SWOE scene model. It has also produced a series of modules which can serve as a basis for development of ∼ comprehensive, dynamic cloud shadowing model. Model upgrades and validation are needed to meet SWOE performance requirements. SSI recommends the following upgrades be implemented:

- Introduce spectral emissivities and albedos into the atmospheric calculations and the energy budget model.

- Use the SSI reflectance model[8] to account for the surface scattering angular dependence, especially with regard to the absorption of solar radiation.

- Generalize the cloud fields to allow translation (wind), growth and inhomogeneity of clouds. Previously developed cloud distribution modules, such as those developed by TASC[9] and ONTAR[10], could be introduced into the shadowing model.

- Calculate skyshine and solar irradiance using the SSI cloud radiance model.[11]

- Account for the finite size of the sun.

- Add Deardorff's water conservation equations[5] to the terrain model.

- Replace the simple single-layer vegetation model currently in TERRAIN with Sparta's forest model.[12]

5. REFERENCES

1. A. Berk, L. S. Bernstein, and D. C. Robertson, "MODTRAN: A Moderate Resolution Model for LOWTRAN 7," Spectral Sciences, Inc. Rpt. No. SSI-TR-154 (April 1989). Prepared for the Geophysics Laboratory (GL-TR-89-0122) under Contract No. F19628-86-C-0079. ADA214337

2. F. X. Kneizys, E. P. Shettle, L. W. Abreu, J. H. Chetwynd, G. P. Anderson, W. O. Gallery, J. E. A. Selby, and S. A Clough, "Users Guide to LOWTRAN 7," AFGL-TR-88-0177, Air Force Geophysics Laboratory, Hanscom AFB, MA 01731 (August 1988). ADA206773

3. T. L. Barnett, "How IRVING (Infrared/Visible Imaging-Numerically Generated) Works: Description of Procedures, Applications, and Submodels in IRVING," JTCG/AS-88-SM-003, Joint Technical Coordinating Group on Aircraft Survivability, Naval Weapons Center (May 1989).

4. Handbook of Geophysics and the Space Environment, A. S. Jursa, Scientific ed., Air Force Geophysics Laboratory (1985). ADA 167000.

5. J. W. Deardorff, "Efficient Prediction of Ground Surface Temperature and Moisture, With Inclusion of a Layer of Vegetation," J. Geophys. Res., 83, 1889 (1978).

6. Boundary Layer Climates, T. R. Oke, 2nd ed. (Methuen & Co., New York, 1987).

7. The Climate Near the Ground, Geiger, R. (Harvard University Press, Cambridge, MA, 1965).

8. D. C. Robertson, "Subroutine Planar: A Semi-Empirical Model for Bi-directional Reflectance," Spectral Sciences, Inc. Rpt. No. SSI-TR-35. Prepared for Aerodyne Research, Inc. under PO No. 2665 (June 1983).

9. M. E. Cianciolo, "Cloud Scene Simulation Model, Version 2.0 Users Guide," TIM-6042-3, TASC, 55 Walkers Brook Drive, Reading, MA 01867 (January 1991).

10. R. Haimes, J. Schroeder, M. Giles, A. Berk, D. Robertson, and B. V. Kessler, "Infrared Cloud Background Model". Proceedings of the Cloud Impacts on DOD Operations and Systems - 1988 Workshop (CIDOS - 88). Held at the Naval Surface Warfare Center, White Oak, MD, 18-20 October 1988. Ed. D. D. Grantham and J. W. Snow.

11. A. Berk, P. K. Acharya, and J. H. Gruninger, "IR Background Clutter Target Signature Model," Spectral Sciences, Inc. Rpt. No. SSI-TR-178. Prepared for NSWC at Dahlgren under Contract No. N60921-90-C-A348.

12. J. R. Hummel, J. R. Jones, D. R. Longtin, and N. L. Paul, "Development of a 3-D Thermal Response Model for Energy Budget and Scene Simulation Studies," LTR-91-002, SPARTA, Inc., 24 Hartwell Avenue, Lexington, MA 02173 (January 1991).